

## *Guazma tomentosa and tribulus terrestris-A mixed green inhibitor for acid corrosion of low carbon steel*

*R. Jeevalatha, R. Sayee Kannan, C. Meenakshi \**

*Department of chemistry, Thiagarajar college, Madurai-625009 Tamilnadu, India*

*Department of Chemistry, Thiagarajar College, Madurai 625009, Tamilnadu, India*

*Department of chemistry, Shri Meenakshi Government arts college for women(A), Madurai, -625002 Tamilnadu, India*

### **Abstract**

*The inhibition performance of acid extracts of mixed inhibitor (Gutle+Tribulus terrestris) on low carbon steel as corrosion inhibitor in 1MHCl and 1MH<sub>2</sub>SO<sub>4</sub> has been studied at different temperatures viz., 303-333K by weight loss method, potentiodynamic polarization and electrochemical impedance spectroscopy measurements. The inhibition efficiency increased with increasing concentration of the inhibitor in both HCl and H<sub>2</sub>SO<sub>4</sub> media. The result of electrochemical measurement confirmed that the inhibitor acts as mixed type of inhibitor. The inhibitive action of mixed inhibitor obeys Langmuir adsorption isotherm. The metal-inhibitor complex can be confirmed by UV-Visible and FTIR spectroscopic studies. The protective film over metal surface was confirmed by scanning electron microscopy (SEM).*

**Keywords-** *Corrosion metal, Inhibition, Potentiodynamic polarization, Electrochemical impedance, SEM, FTIR, Uv-Visible spectroscopy.*

### **1. Introduction**

Low carbon steel and its alloys are widely used in various industrial processes could be corroded during the acidic application particularly with the use of H<sub>2</sub>SO<sub>4</sub> and HCl medium. Acid solution used in various operation such as acid pickling, descaling, industrial acid cleaning and oil well acidizing [1]. During several decades many techniques have been implemented to reduce the corrosion of low carbon steel due to attack by acids. One of the present techniques for reducing the corrosion is the use of environment friendly green inhibitor. Many of the green inhibitor is based on organic compound containing N, S, O, and P atoms and conjugate bonds in the molecule that facilitate adsorption on the metal surface [2,3]. Most of the green inhibitor are environment friendly, non-toxic, biodegradable, inexpensive and readily available in plenty [4]. Corrosion inhibition on natural compounds extracted from leaves or seeds as green inhibitors have been reported by various authors [5-12]. Some organic compounds like ascorbic acid [13], Succinic acid [14], caffeine [15], pennyroyal oil [16], amino acid [17], tryptamine [18] and caffeic acid [19] have been used for corrosion inhibition of metals.

The aim of the present study is to find a cheap, inexpensive, safe and environmental friendly substances that could be used as corrosion inhibition for low carbon steel in different acidic medium. In this present work, it has been found that the corrosion of low carbon steel in 1MHCl and 1MH<sub>2</sub>SO<sub>4</sub> using the extract of (Guazma tomentosa and Tribulus Terrestris) as mixed

inhibitor by mass loss method, electrochemical measurements, FTIR, SEM, EDS spectroscopic analysis [20].

Guazma tomentosa (Gutle) and Tribulus terrestris (TTLE) is a well-known and easily available plant in India. 'Gutle' belongs to Sterculiaceae family and TTLE belongs to Zygophyllaceae family. The phytochemical component of Gutle are colistin, colatannins, catechins, caffeine, kaempferol, procyanidin B-2, procyanidin B-5, procyanidin C-1, tartaric acid, xanthan gum and TTLE are steroidal saponins compounds, polysaccharides and tannins. No reported literature is available for this combination of (Gutle + TTLE) inhibitor for controlling the corrosion of low carbon steel in 1M HCl and 1M H<sub>2</sub>SO<sub>4</sub>.

## 2. Experimental

### 2.1. Preparation of the sample

Low carbon steel coupon of the composition C: 1.83%, Fe: 2.66%, Cr: 0.06% were used for the present work. Low carbon steel of specimen of the size of 2.5 X 2.5 X 0.4 cm dimensions were used for mass loss method, while specimen of the size of 0.5 cm<sup>2</sup> was used for electrochemical studies. The specimens were degreased by washing with acetone at room temperature and stored in a desiccators'.

### 2.2. Preparation of the mixed inhibitor (Gutle+TTLE)

Guazma tomentosa and Tribulus Terrestris leaves were collected in and around Virudhunagar district, Tamilnadu. The leaves were dried and ground into powdered form. About 10g of each powdered leaves were extracted with absolute ethanol in Soxhlet apparatus for 5 hrs. After completion of the extraction, it was filtered and concentrating the residue by heating in a water bath at 55°C. From the respective stock residue, the test solutions were prepared in the concentration range of 0.05, 0.1, 0.15, 0.2, 0.25 g/l.

### 2.3. Mass loss experiment

Mass loss experiment were conducted at various temperature in the range of 303K-333K in 1M HCl & 1M H<sub>2</sub>SO<sub>4</sub>. The weighed and polished low carbon steel specimens were immersed in 100ml of the mixed inhibitor solution with the different concentration of 0-250mg/l for 2 hrs. After 2 hrs, the specimens were taken, washed with distilled water and acetone and then reweighed. The mass loss ( $\Delta M$ ) and the inhibition efficiency (%IE) were calculated using the following relation

$$CR = 534 X \frac{\Delta M}{DST} \quad (1)$$

$$IE\% = \frac{M_{Lo} - M_{Li}}{M_{Lo}} X 100 \quad (2)$$

Here  $\Delta M = (M_{Lo} - M_{Li})$ , where  $M_{Lo}$  and  $M_{Li}$  are the mass loss of low carbon steel in the absence and presence of inhibitor.  $D$  is the density of the iron rod (g/cm<sup>3</sup>),  $A$  is the Area of the specimen in inch<sup>2</sup> and  $T$  is the immersion period in hours.

### 2.4. Electrochemical Measurement

Nyquist impedance curves and Tafel polarization curves were recorded using electrochemical workstation impedance analyzer model CH1760D. A cell assembles three compartments of

electrode used. The polished low carbon steel with the exposed area of  $0.5\text{cm}^2$  was immersed in a mixed inhibitor solution. A platinum as counter electrode and reference as saturated calomel electrode were used for this electrochemical cell. All electrochemical measurement were carried out at 303K using 100ml of the mixed inhibitor ( $1\text{MHCl}$  &  $1\text{MH}_2\text{SO}_4$ ) solution in stationary condition [21] Before each potentiodynamic polarization and electrochemical impedance measurements, the electrode was immersed in the mixed inhibitor solution to corrode freely and its open circuit potential was recorded [22]. Potentiodynamic polarization were recorded from  $-250\text{mV}$  to  $+250\text{mV}$  with the scan rate of  $0.01\text{v/s}$ . The electrochemical impedance spectroscopy measurements were recorded in the frequency range of  $0.1\text{-}1\text{Hz}$ . Each experiment was repeated to triplicate to check the reproducibility of the data.

### 3. Surface Analysis

#### 3.1. FTIR Studies

The formation of protective film over the surface of the low carbon steel specimen was examined by carrying out FTIR spectroscopic investigations. FTIR spectrum was recorded on BRUKER spectrometer in the IR range of  $4000\text{-}400\text{cm}^{-1}$ . The FTIR spectrum of protective film on the surface of low carbon steel was recorded by carefully removing the film, mixing it with KBr & making the pellets as per standard earlier [23-25]. The FTIR spectra of extract residue and the mixed inhibitor film adsorbed over low carbon steel surface were compared for its adsorptive studies.

#### 3.2. UV-Visible Spectroscopy

The adsorption behaviour of organic compounds present in the extract were analysed with the help of UV-Visible spectrum. The UV-Visible absorption spectra obtained on (JASCO W 32 spectrophotometer) low carbon steel surface can be analysed with the help of quartz glass cell on  $400\text{-}800\text{nm}$ . Absorption spectra of mixed inhibitor (Gutle + TTLE) residue and the test solution with specimen immersed in additive were compared to investigate its adsorption nature [26].

#### 3.3. Scanning Electron Microscopy & EDAX analysis

The low carbon steel specimens were immersed in acidic medium of  $1\text{MHCl}$  &  $1\text{MH}_2\text{SO}_4$  in the absence and presence of optimum concentration of mixed inhibitor for a period of 24hrs. After 24hrs, the specimens were taken out and dried. The nature of the protective film formed on the surface of the low carbon steel was examined by using a BRUKER SEM analysis with EDS Spectrometer.

## 4. Result and Discussion

### 4.1. Mass loss experiment

The corrosion rate and inhibition efficiency of low carbon steel in  $1\text{MHCl}$  &  $1\text{MH}_2\text{SO}_4$  in the uninhibited and inhibited mixed extract solution of different concentrations were determined at  $303\text{K}\text{-}333\text{K}$ . Fig (1,2) & (3,4) shows the concentration effect of mixed inhibitor (Gutle + TTLE) on the corrosion rate and inhibition efficiency of  $1\text{MHCl}$  &  $1\text{MH}_2\text{SO}_4$  in the presence and absence of leaves extract. From the graph, it is confirmed that the corrosion rate of low

carbon steel decreased in the presence of inhibitor then its absence in the acidic solution. The corrosion rate can also decreased with the increasing concentration of mixed inhibitor indicates that the corrosion of low carbon steel was inhibited by Gutle+ TTLE leaves extract in 1MHCl & 1MH<sub>2</sub>SO<sub>4</sub>. The maximum inhibition efficiency of 1MHCl was attained to be 90% and 1MH<sub>2</sub>SO<sub>4</sub> was 86% at 250mg/l(303K) which can be confirmed that the mixed inhibitor was a very good inhibitor in both the acid media. In Fig (5)&(6) shows the plot of inhibition efficiency Vs temperature with different concentrations of mixed inhibitor. From the graph ,it is clear that inhibition efficiency decreased with the increase of temperature, which can be confirmed that the desorption of mixed inhibitor on the low carbon steel surface [27-33].In Fig (7) & (8) shows the variation of time with corrosion rate on low carbon steel in 1MHCl & 1MH<sub>2</sub>SO<sub>4</sub> with the different concentration of inhibitor.

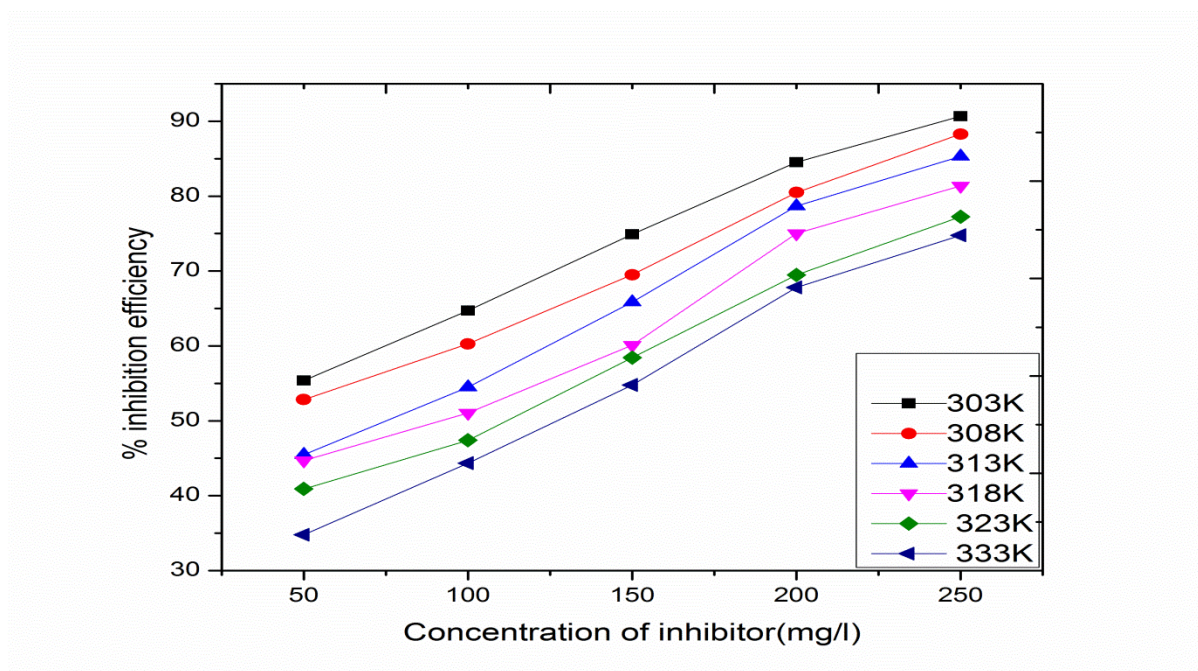


**Figure.1. Variation of inhibition efficiency of low carbon steel with and without mixed inhibitor in 1MHCl at different temperature**

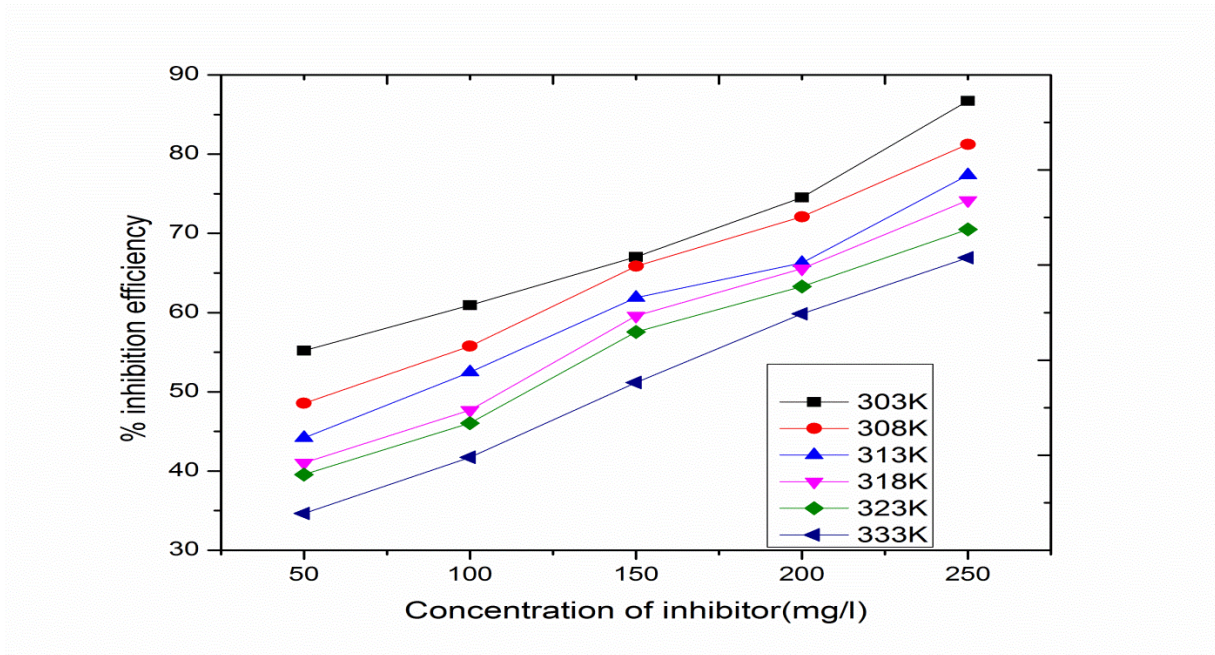


Figure .2. Variation of inhibition efficiency of low carbon steel with and without mixed inhibitor in 1M H<sub>2</sub>SO<sub>4</sub> at different temperature

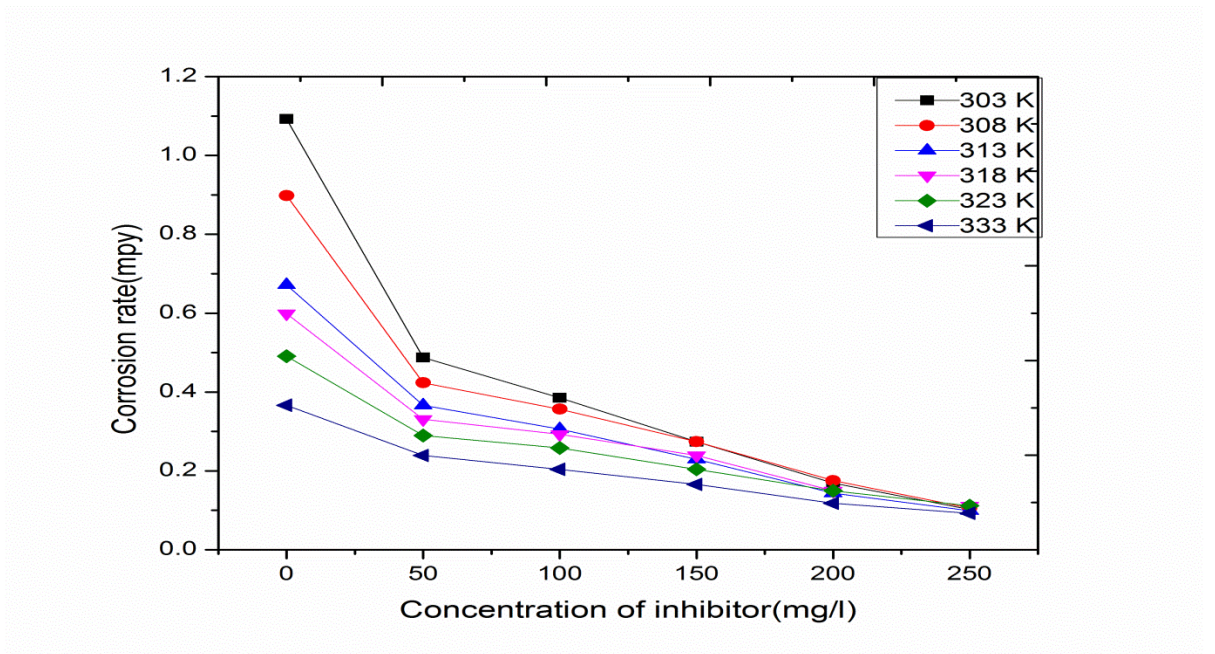


Figure.3. Corrosion rate of low carbon steel in 1MHCl with and without mixed inhibitor

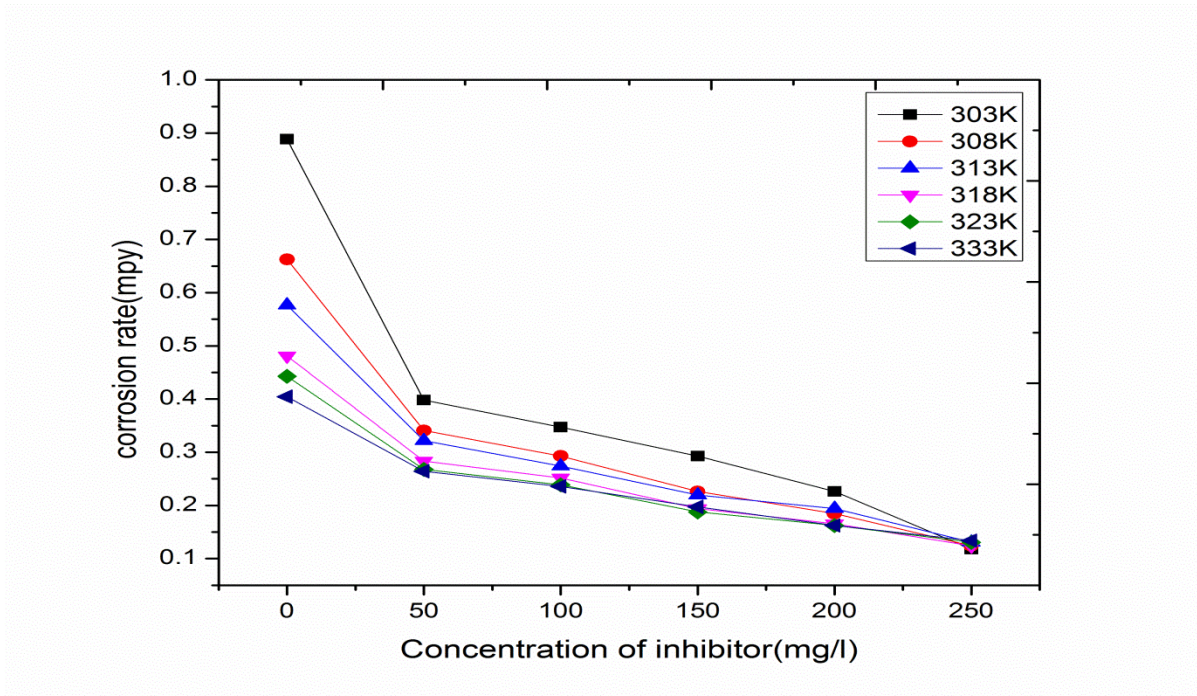


Figure .4. Corrosion rate of low carbon steel in 1M H<sub>2</sub>SO<sub>4</sub> with and without mixed inhibitor

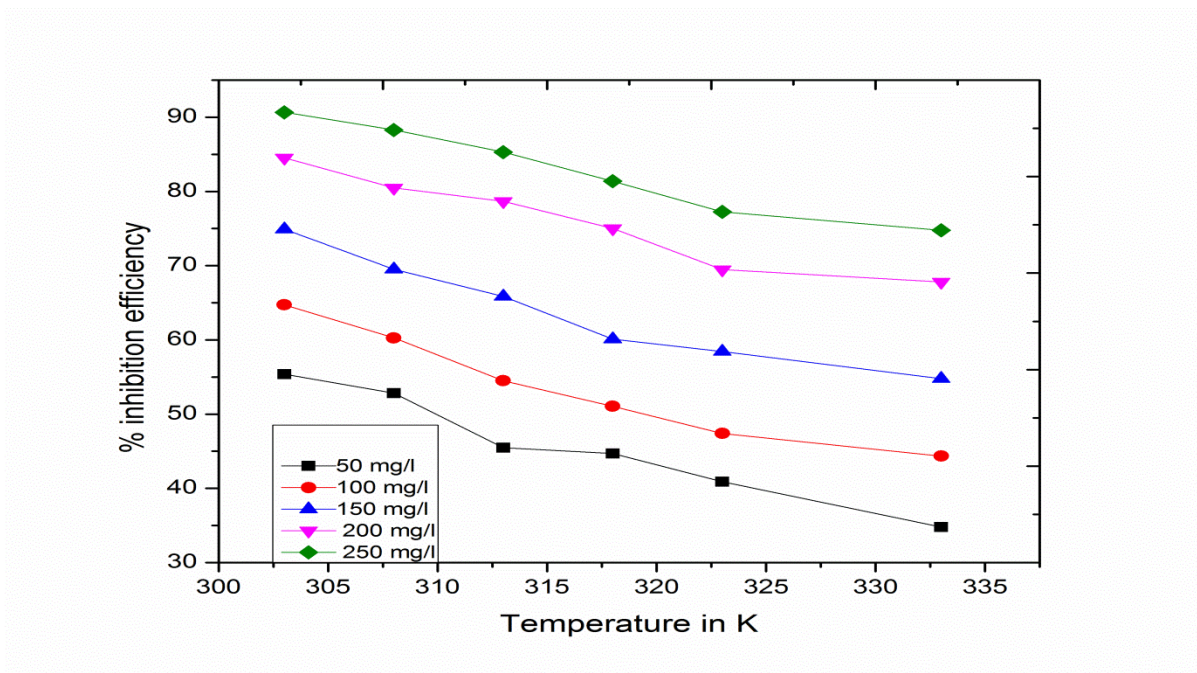


Figure .5. Inhibition Efficiency with temperature in the presence of different concentration of mixed inhibitor(1M HCl)

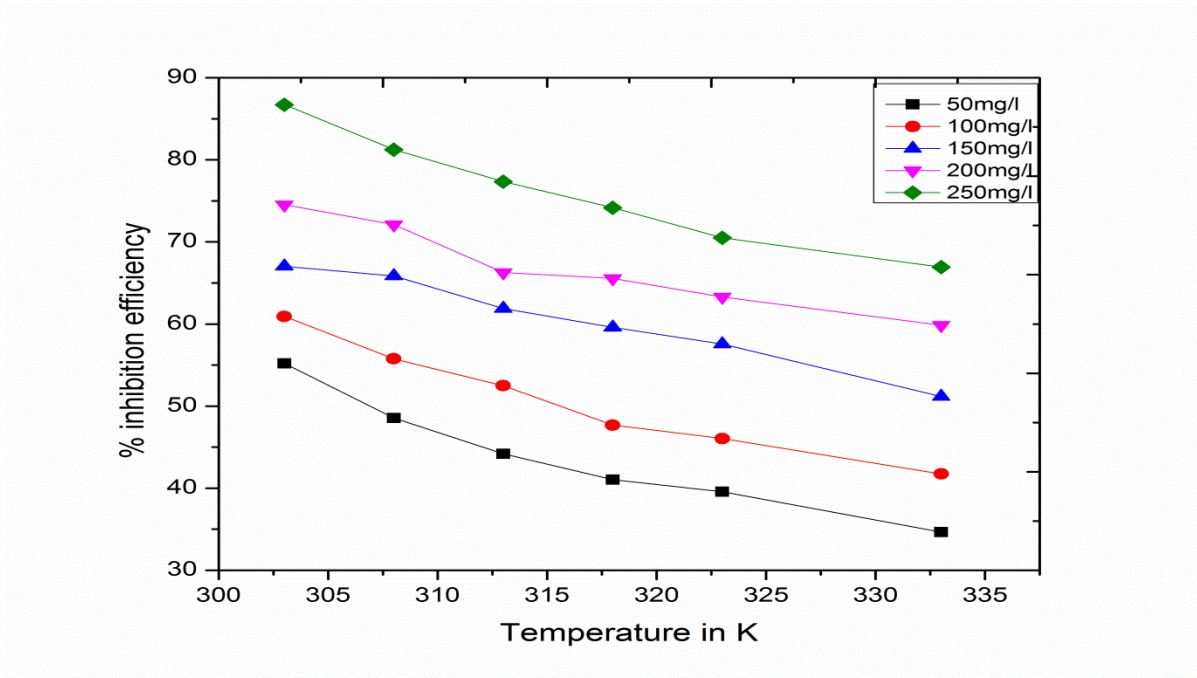


Figure .6. Inhibition Efficiency with temperature in the presence of different concentration of mixed inhibitor (1M H<sub>2</sub>SO<sub>4</sub>)

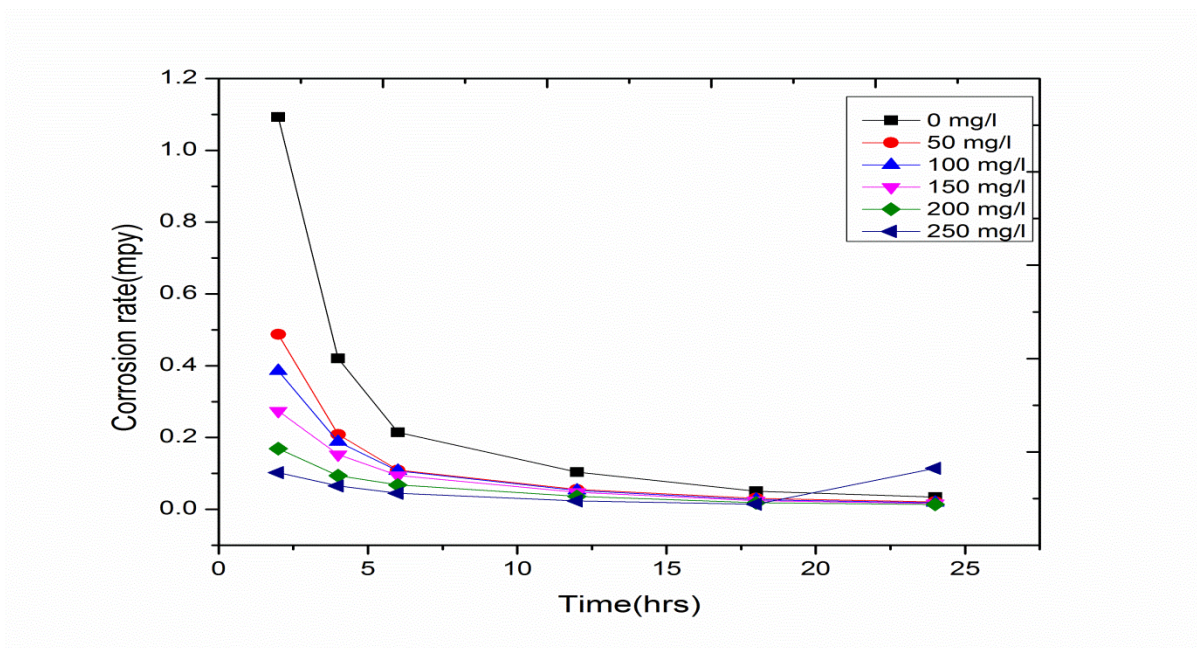
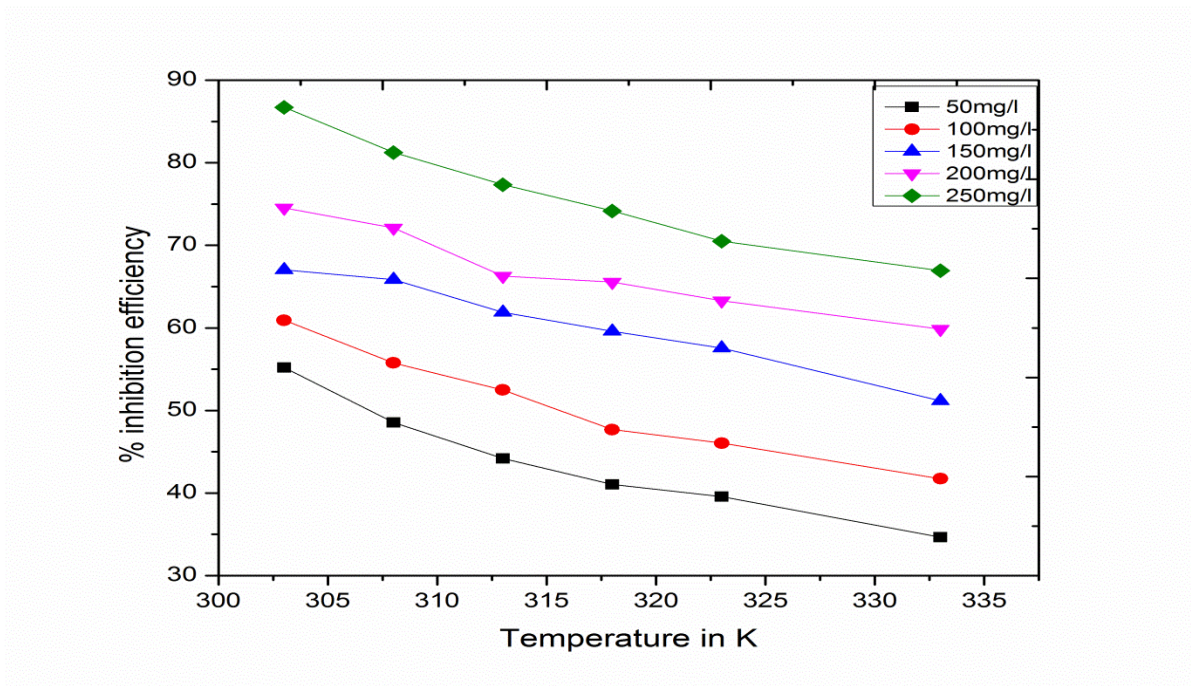


Figure .7. Corrosion rate of mixed inhibitor as a function of time in 1M HCl



**Figure .8. Corrosion rate of mixed inhibitor as a function of time in 1MH<sub>2</sub>SO<sub>4</sub>**

**4.2. Electrochemical measurements**

**4.2.1. Potentiodynamic polarization studies**

The potentiodynamic polarization curves of low carbon steel in 1MHCl and 1MH<sub>2</sub>SO<sub>4</sub> with the varying concentrations of mixed inhibitor is shown in Fig (9) & (10). The corrosion kinetic parameters such as corrosion potential ( $E_{corr}$ ), Corrosion current density ( $I_{corr}$ ), anodic tafel slope ( $b_a$ ) and cathodic tafel slope ( $b_c$ ), linear polarization (LPR) and inhibition efficiency are deduced from the curves of 1MHCl and 1M H<sub>2</sub>SO<sub>4</sub> are given in the table (1) & (2). The inhibition efficiency is calculated using the following relation

$$IE\% = \left( i_{corr}^o - \frac{i_{corr}}{i_{corr}^o} \right) \times 100 \quad (3)$$

Where  $i_{corr}^o$  and  $i_{corr}$  are the corrosion current density values in the absence and presence of inhibitor. The increase in concentration of the mixed inhibitor decreases the  $I_{corr}$  values. The addition of mixed inhibitor on acid corrosion of low carbon steel in both the acid media, do not show any appreciable shift in  $E_{corr}$  which imply that the analyzed extract act as a mixed type of inhibitor [34]. The values of  $b_c$  was changed less than  $b_a$  values, it is confirmed that anodic reaction was controlled predominantly than the cathodic one at all concentrations. In the presence of inhibitor system, the corrosion current decreased from (1MHCl) 742 to 79 mA cm<sup>-2</sup> and in 1MH<sub>2</sub>SO<sub>4</sub> from 690 to 94 mA cm<sup>-2</sup> and this observation suggests that addition of mixed inhibitor to both 1MHCl and 1MH<sub>2</sub>SO<sub>4</sub> solution will reduce anodic dissolution of low carbon steel more than the cathodic hydrogen evolution reaction [35].

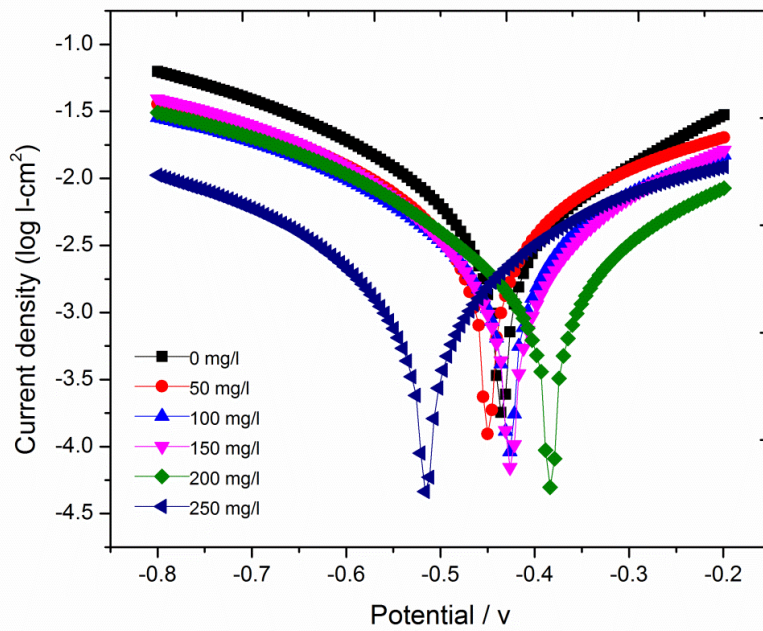


Figure.9. Tafel plot of low carbon steel immersed in 1M HCl with and without *Mixed inhibitor*

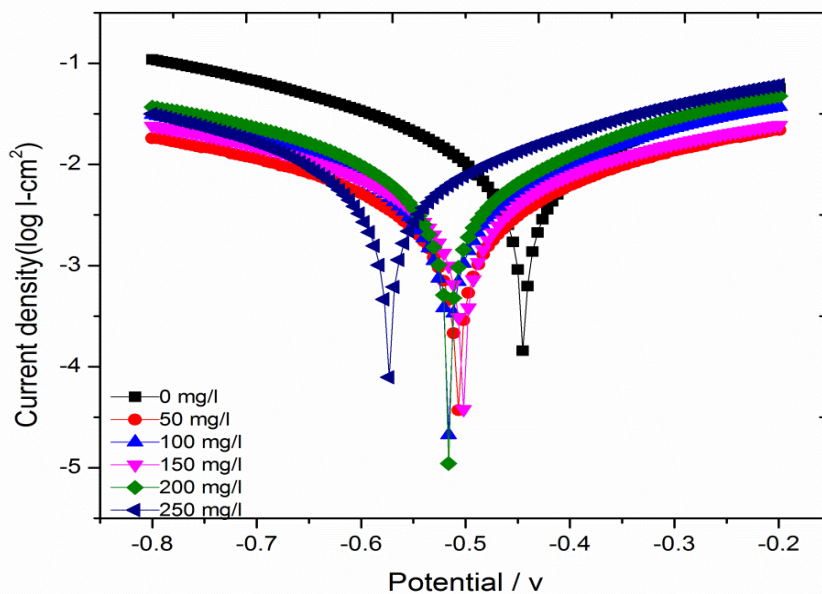


Figure.10. Tafel plot of low carbon steel immersed in 1M H<sub>2</sub>SO<sub>4</sub> with and without *Mixed inhibitor*

**Table .1. Potentiodynamic polarization parameters for the corrosion of low carbon steel in 1MHCl containing different Concentrations of Mixed inhibitor**

$C_{inh}(mg/l)$	$E_{corr}(mV)$	$I_{corr}(mA\ cm^{-2})$	$-b_c(mV\ decade^{-1})$	$-b_a(mV\ decade^{-1})$	$R_p(\Omega cm^2)$	%IE
0	-374	742	141.3	137.6	24.48	-
50	-390	209	139.4	134.2	7.03	71.8
100	-403	175	137.1	131.8	5.98	76.4
150	-415	139	133.7	129.4	4.86	81.2
200	-430	114	127.3	126.2	4.13	84.6
250	-433	79	125.5	124.3	2.90	89.3

**Table .2. Potentiodynamic polarization parameters for the corrosion of low carbon steel in 1M $H_2SO_4$  containing different Concentrations of Mixed inhibitor**

$C_{inh}(mg/l)$	$E_{corr}(mV)$	$I_{corr}(mA\ cm^{-2})$	$-b_c(mV\ decade^{-1})$	$-b_a(mV\ decade^{-1})$	$R_p(\Omega cm^2)$	%I
0	-384	640	137.1	134.3	23.3	-
50	-443	272	135.3	131.5	9.38	60.6
100	-467	205	133.5	128.2	7.20	63.8
150	-442	165	129.4	126.3	5.94	76.1
200	-495	123	127.2	125.2	4.48	82.2
250	-410	94	124.7	123.4	3.48	86.4

#### 4.2.2. Electrochemical impedance measurement

Impedance behaviour of low carbon steel in 1M $HCl$  and 1M $H_2SO_4$  in the presence and absence of the inhibitor is shown in the fig (11) & (12).The impedance parameters such as  $R_{ct}$ ,  $C_{dl}$  and  $f_{max}$  derived from nyquist plots are given in the table (3) & (4).The charge transfer values are decreased with increasing concentration of the inhibitor indicating that,the process is mainly

controlled by the corrosion low carbon steel. In the impedance studies, the inhibition efficiency is calculated as

$$IE\% = (R_{ct(inh)} - R_{ct}) / R_{ct(inh)} \times 100 \quad (4)$$

Where  $R_{ct}$  and  $R_{ct(inh)}$  are uninhibited and inhibited charge transfer resistance respectively. The diameter of Nyquist plots increased on increasing the concentration of mixed inhibitor which indicating that the strengthening of inhibitor film on the metal surface [36]. The values of  $R_{ct}$  in the inhibited substrates was increased with the increasing concentration of inhibitors. The values of  $C_{dl}$  are decreased with increasing in inhibitor concentration and it was due to the adsorption of mixed inhibitor on the metal surface leading to the formation of a protective layer on the electrode surface and decreased the extent of dissolution reaction [37]. The inhibition efficiencies calculated from EIS showed good agreement with the results obtained from polarization methods and could be attributed to decreased local dielectric constant and increased thickness of the electrical double layer [38].

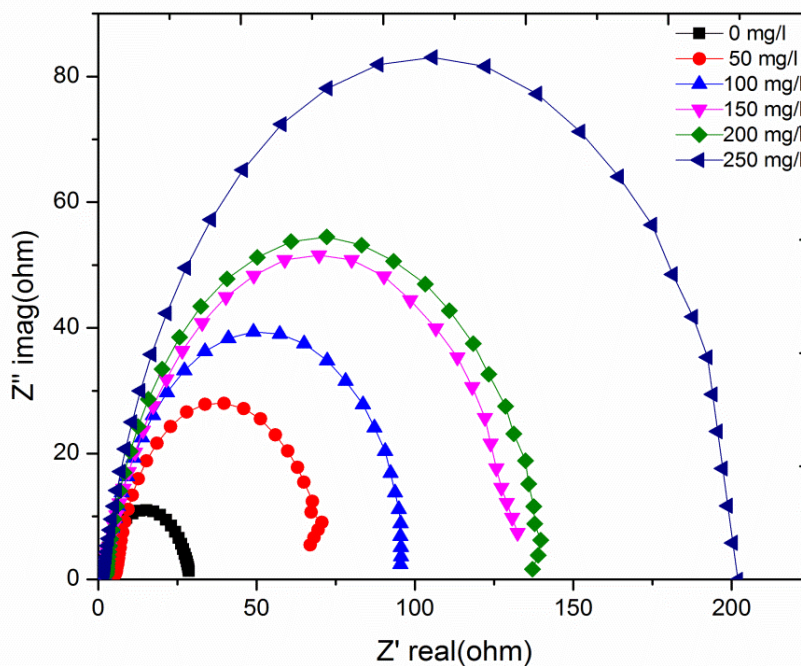


Figure .11. Nyquist plot of low carbon steel immersed in 1M HCl with different concentration of *Mixed inhibitor* at 303K

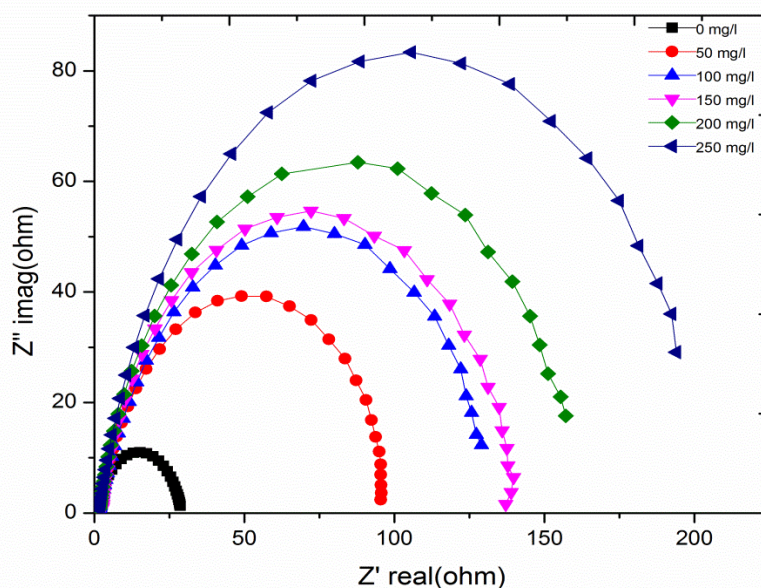


Figure .12.Nyquist plot of low carbon steel immersed in 1MH<sub>2</sub>SO<sub>4</sub> with different concentration of *Mixed inhibitor* at 303K

Table. 3. Electrochemical impedance parameters for low carbon steel in 1M HCl in the absence and presence of *Mixed inhibitor*

$C_{inh}(mg\ l^{-1})$	$R_{ct}(\Omega\ cm^2)$	$C_{dl}(F\ cm^{-2})$	%IE
0	28.1	437	-
50	67.3	95	58.2
100	95.6	83	70.6
150	132.4	71	78.7
200	139.7	65	79.8
250	200.4	52	85.9

**Table .4.Electrochemical impedance parametres for low carbon steel in 1M H<sub>2</sub>SO<sub>4</sub> in the absence and presence of Mixed inhibitor**

C <sub>inh</sub> (mg l <sup>-1</sup> )	R <sub>ct</sub> (Ω cm <sup>2</sup> )	C <sub>dl</sub> (F cm <sup>-2</sup> )	%IE
0	28.5	470	-
50	95.6	90	70.1
100	129	78	77.9
150	138.9	69	79.4
200	157	64	81.8
250	201	55	85.8

## 5. Adsorption isotherm

Adsorption isotherm provide an important information on interaction of mixed inhibitor and the low carbon steel surface [39].Surface coverage data play an important role in characteristics of inhibitor and they are useful for fitting to various isotherm including Langmuir, freundlich, Tempkin isotherm. Mixed inhibitor(Gutle + TTLE) in both HCl and H<sub>2</sub>SO<sub>4</sub> obeys Langmuir adsorption isotherm by giving a straight line for the plot of C vs C/Θ, which is given as Fig(13) &(14).

$$\frac{C}{\theta} = \frac{1}{K_{(ads)}} + C \quad (5)$$

Where C is the Concentration of mixed inhibitor(mg/l),K is the adsorption –desorption equilibrium constant and Θ is the surface coverage which is given as[40]

$$\theta = \% \frac{IE}{100} \quad (6)$$

The adsorption behaviour indicated that the adsorption of mixed inhibitor on both 1MHCl and 1MH<sub>2</sub>SO<sub>4</sub> medium of low carbon steel surface obeyed Langmuir adsorption isotherm meaning that there was no interaction between the adsorbed species[41].The free energy of adsorption (ΔG<sub>ads</sub>) and the equilibrium constant (K) are related by the following equation.

$$\Delta G_{ads} = -RT \ln(55.5K) \quad (7)$$

Here R is the gas constant, T is the absolute temperature and 55.5 is the concentration of water in the solution.

The value of K were found to decrease in both the acid medium with increasing temperature and it can be showing that the interaction between the adsorbed molecules and low carbon steel surface have weak vanderwaals force of attraction. Such data can explain the decrease in protection efficiency with increasing temperature [42].

The values of  $\Delta G_{\text{ads}}$  and K were listed in Table (5) & (6) . The values of  $\Delta G_{\text{ads}}$  was less than the -20KJ in both the acid medium and it can be suggests physisorption mechanism which was consistent with electrostatic interaction between inhibitor molecules and the low carbon steel surface [43,44].

**Table.5.Langmuir adsorption parameters and free energy of adsorption of mixed inhibitor on the surface of low carbon steel in 1MHCL**

Temp(K)	$\Delta G_{\text{ads}}$	K	$-\Delta H_{\text{ads}}^{\circ}(\text{kJ mol}^{-1})$	$-\Delta S_{\text{ads}}^{\circ}(\text{J mol k}^{-1})$	R <sup>2</sup>
303	36.30	1.7	$1.56 \times 10^{-3}$	0.05	0.98
308	21.46	1.5	$1.62 \times 10^{-3}$	1.17	0.96
313	16.41	1.2	$1.69 \times 10^{-3}$	3.31	0.95
318	15.02	1.1	$1.69 \times 10^{-3}$	3.84	0.93
323	12.22	1.0	$1.70 \times 10^{-3}$	4.65	0.92
333	10.36	0.08	$1.73 \times 10^{-3}$	6.44	0.91

**Table.6.Langmuir adsorption parameters and free energy of adsorption of mixed inhibitor on the surface of low carbon steel in 1MH<sub>2</sub>SO<sub>4</sub>**

Temp(K)	$\Delta G^{\circ}_{ads}$	K	$-\Delta H^{\circ}_{ads}(kJ\ mol^{-1})$	$-\Delta S^{\circ}_{ads}(J\ mol\ k^{-1})$	R <sup>2</sup>
303	78.98	1.7	$1.57 \times 10^{-3}$	0.24	0.94
308	74.84	1.4	$1.64 \times 10^{-3}$	1.57	0.96
313	48.65	1.3	$1.65 \times 10^{-3}$	2.52	0.95
318	19.21	1.1	$1.66 \times 10^{-3}$	3.80	0.95
323	12.52	1.1	$1.69 \times 10^{-3}$	3.87	0.96
333	12.10	0.09	$1.70 \times 10^{-3}$	5.77	0.94

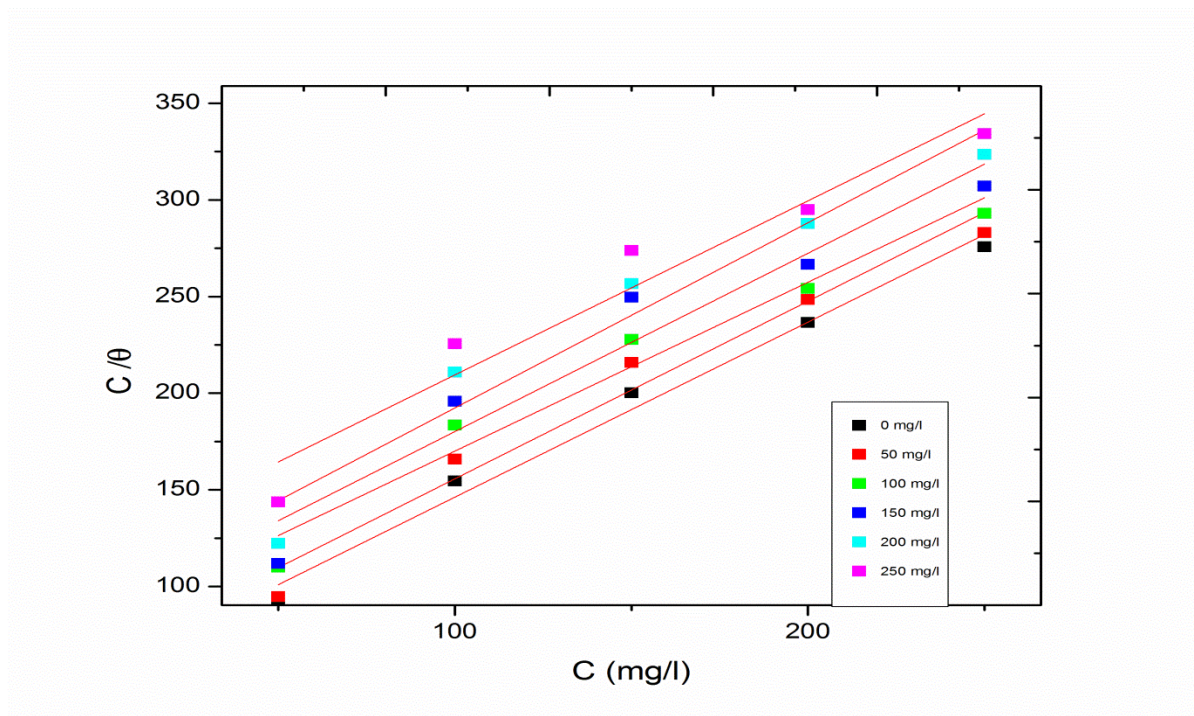


**Figure.13.Langmuir adsorption isotherm plot for low carbon steel in 1MHCl with mixed inhibitor extract at different temperature**

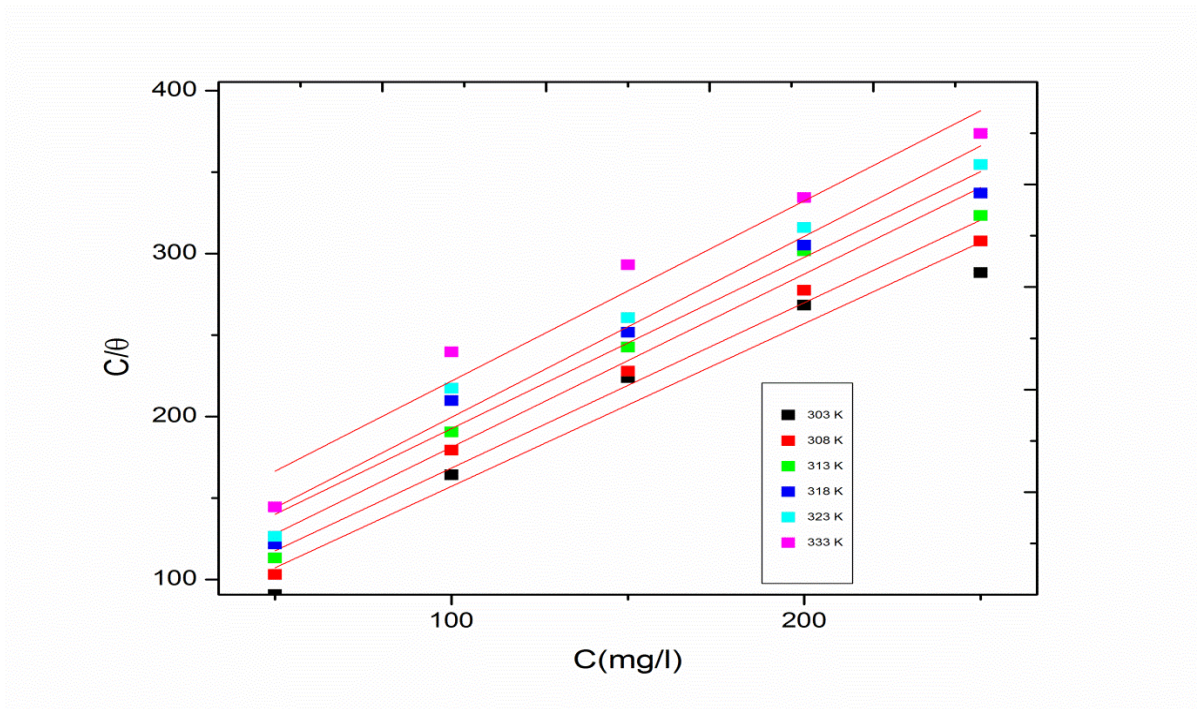


Figure.14.Langmuir adsorption isotherm plot for low carbon steel in 1M<sub>H2</sub>SO<sub>4</sub> with mixed inhibitor extract at different temperature

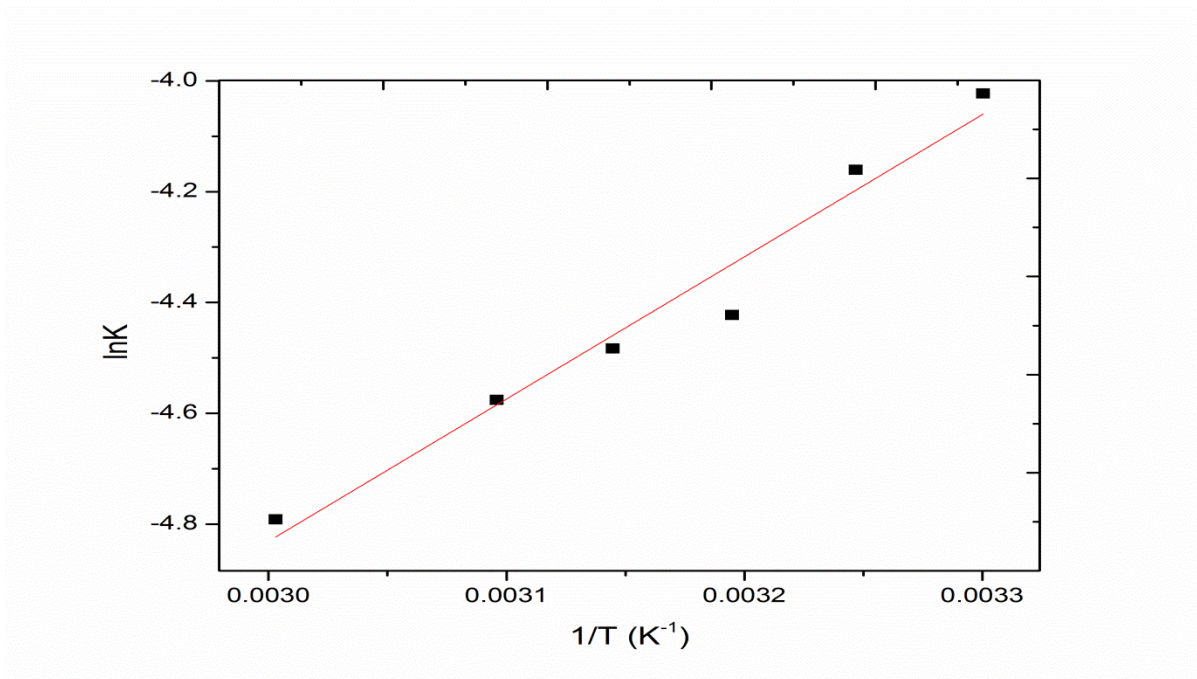
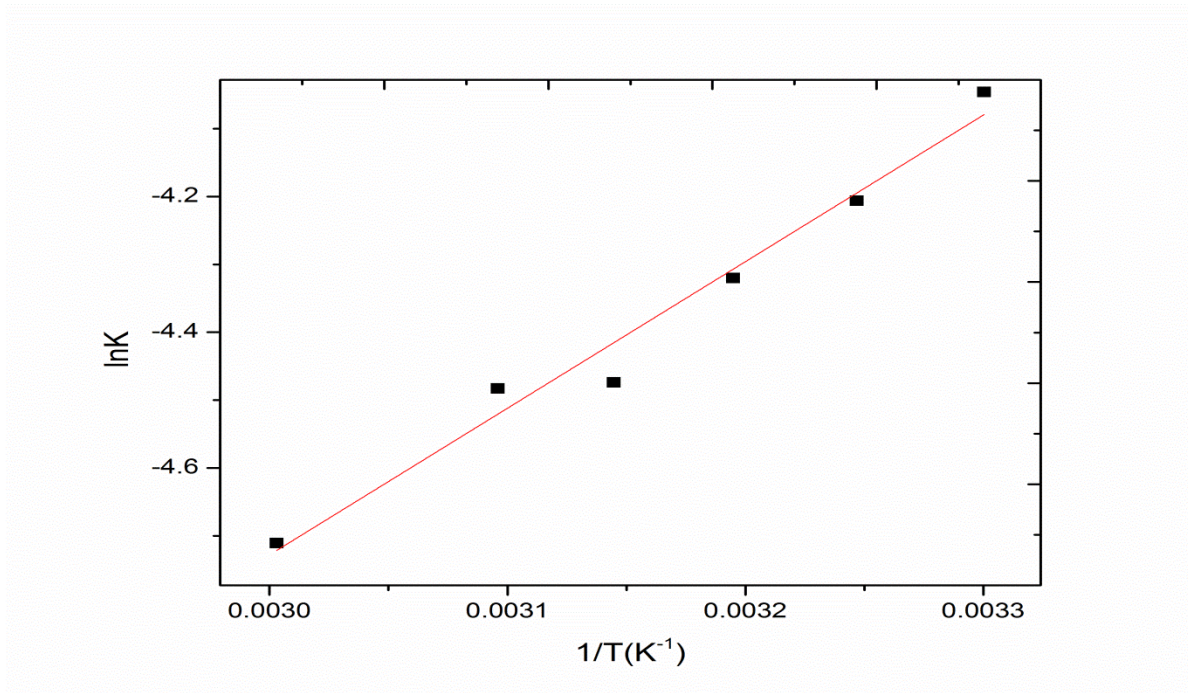


Figure .15.Plot of  $\ln K$  vs  $1/T$  for the adsorption of mixed inhibitor at lowcarbon steel /HCL interface



**Figure .16. Plot of  $\ln K$  vs  $1/T$  for the adsorption of mixed inhibitor at low carbon steel /  $H_2SO_4$  interface**

The entropy of adsorption and the heat of adsorption are important values for understanding adsorption of mixed inhibitor molecules at metal/solution interface. The heat of adsorption ( $\Delta H_{ads}$ ) is calculated using the Van't Hoff equation

$$\ln K = -\Delta H_{ads}/RT + Constant \quad (8)$$

Fig (15) & (16) gives the straight lines of plot of  $\ln K$  vs  $1/T$  and the straight line is equal to  $-\Delta H_{ads}/R$ . The standard entropy of activation ( $\Delta S_{ads}$ ) is obtained by the thermodynamic equation

$$\Delta S_{ads} = \frac{\Delta G_{ads} - \Delta H_{ads}}{T} \quad (9)$$

The value of  $\Delta H_{ads}$  are negative and it indicates that the adsorption of mixed inhibitor is an exothermic process and it is due to the gradual desorption of mixed inhibitor from the low carbon surface. The  $\Delta S_{ads}$  values are negative and it can be explained that, before the adsorption of inhibitor molecules into the low carbon steel surface, inhibitor molecules might freely move in the bulk solution (inhibitor molecules were chaotic), but with the process of adsorption, inhibitor molecules were orderly adsorbed onto the steel surface, as a result a decrease in entropy is observed [45].

## 6. Thermodynamic consideration

The thermodynamic parameters like enthalpy of activation  $\Delta H^*$ , entropy of activation  $\Delta S^*$  and the activation energy  $E_a$ , for corrosion of low carbon steel in 1M HCl and 1M  $H_2SO_4$  solution in the absence and presence of mixed inhibitor (Gutle + TTLE) at 303K to 333K were calculated from Arrhenius Equation [46].

$$CR = A \exp\left(-\frac{E_a}{RT}\right) \quad (10)$$

The formula of activated complex from the enthalpy and entropy change in the transition state was obtained from the transition state equation

$$CR = \left\{ \left( \frac{\log R}{Nh} + \frac{\Delta S^*}{2.303} \right) \right\} \frac{-\Delta H^*}{2.303RT} \quad (11)$$

**Table.7. Kinetic parameters for corrosion of low carbon steel in 1M HCL in the absence and presence of different concentrations of mixed inhibitor**

$C_{inh}(mg\ l^{-1})$	$E_a(kJ\ mol^{-1})$	$\Delta H^*(kJ\ mol^{-1})$	$-\Delta S^*(J\ mol\ k^{-1})$
0	1.39	14.38	197.58
50	9.67	32.35	197.58
100	14.30	44.72	197.57
150	17.71	92.97	197.57
200	19.98	1	48.56
250	30.71	169.36	197.56

**Table.8. Kinetic parameters for corrosion of low carbon steel in 1M H<sub>2</sub>SO<sub>4</sub> in the absence and presence of different concentrations of mixed inhibitor**

$C_{inh}(mg\ l^{-1})$	$E_a(kJ\ mol^{-1})$	$\Delta H^*(kJ\ mol^{-1})$	$-\Delta S^*(J\ mol\ k^{-1})$
0	3.06	13.81	197.58
50	8.81	20.65	197.58
100	10.42	22.80	197.57
150	10.59	26.85	197.57
200	11.67	63.64	197.57
250	21.63	66.96	197.56

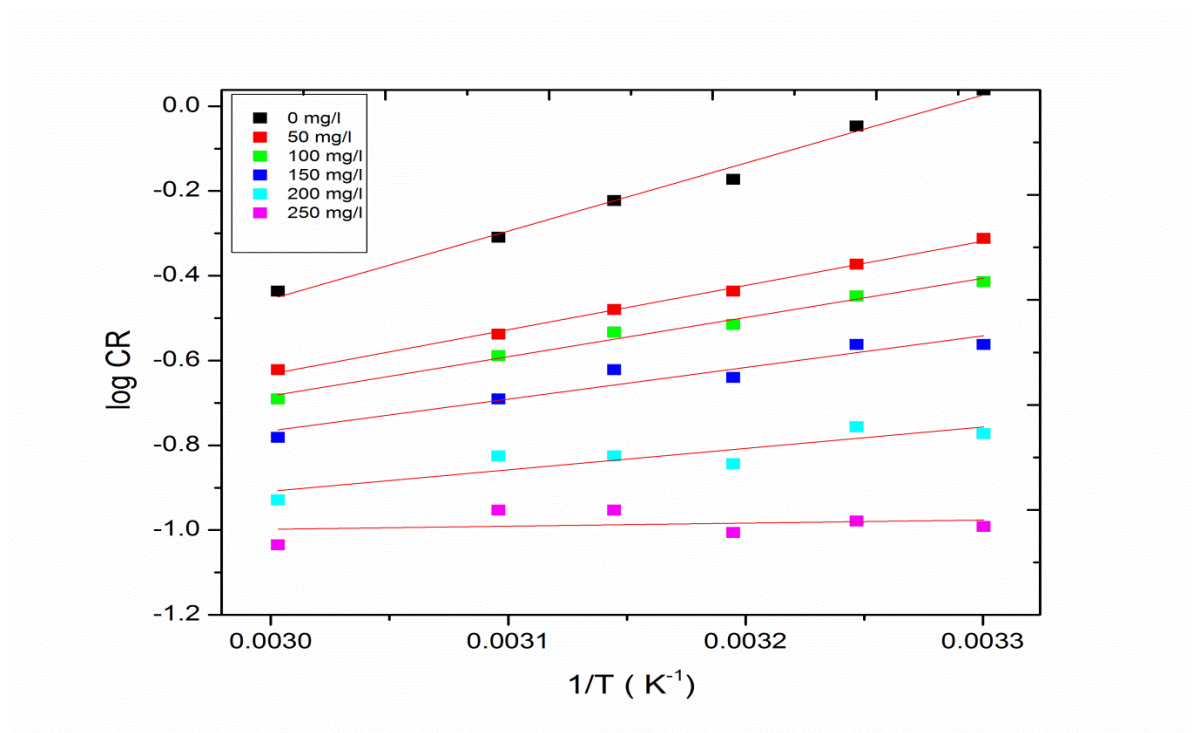


**Figure .17. Arrhenius plot for low carbon steel in 1M HCl in the absence and presence of different concentration of mixed inhibitor**

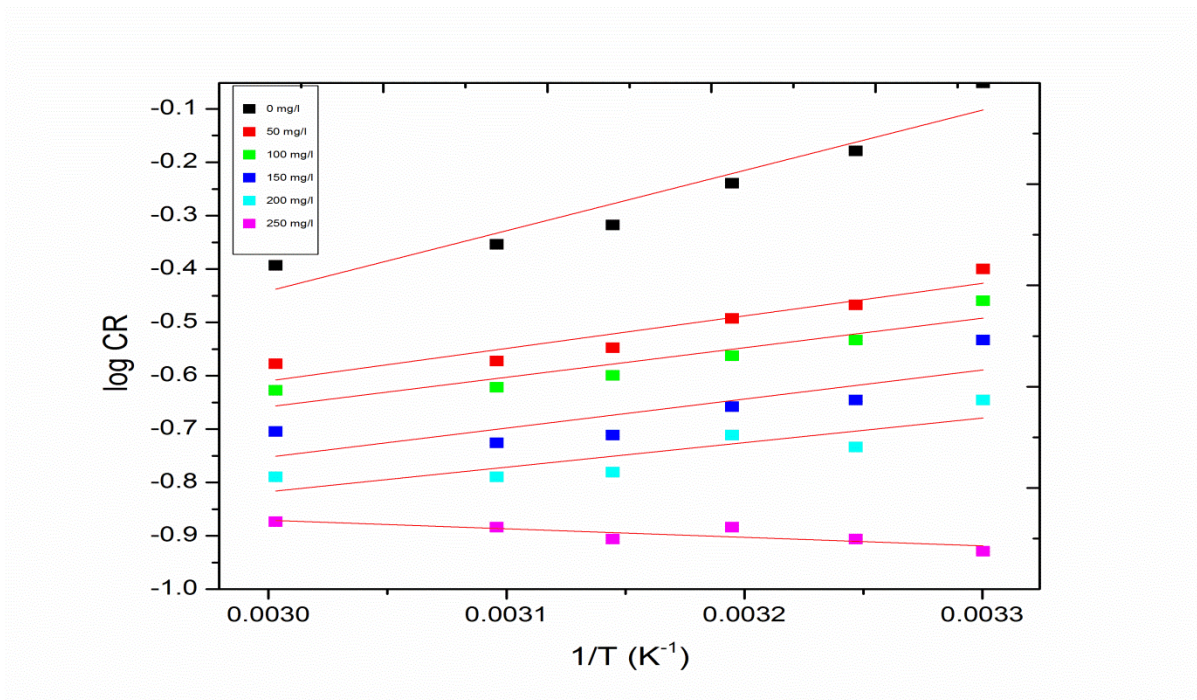


Figure.18. Arrhenius plot for low carbon steel in 1M H<sub>2</sub>SO<sub>4</sub> in the absence and presence of different concentration of mixed inhibitor

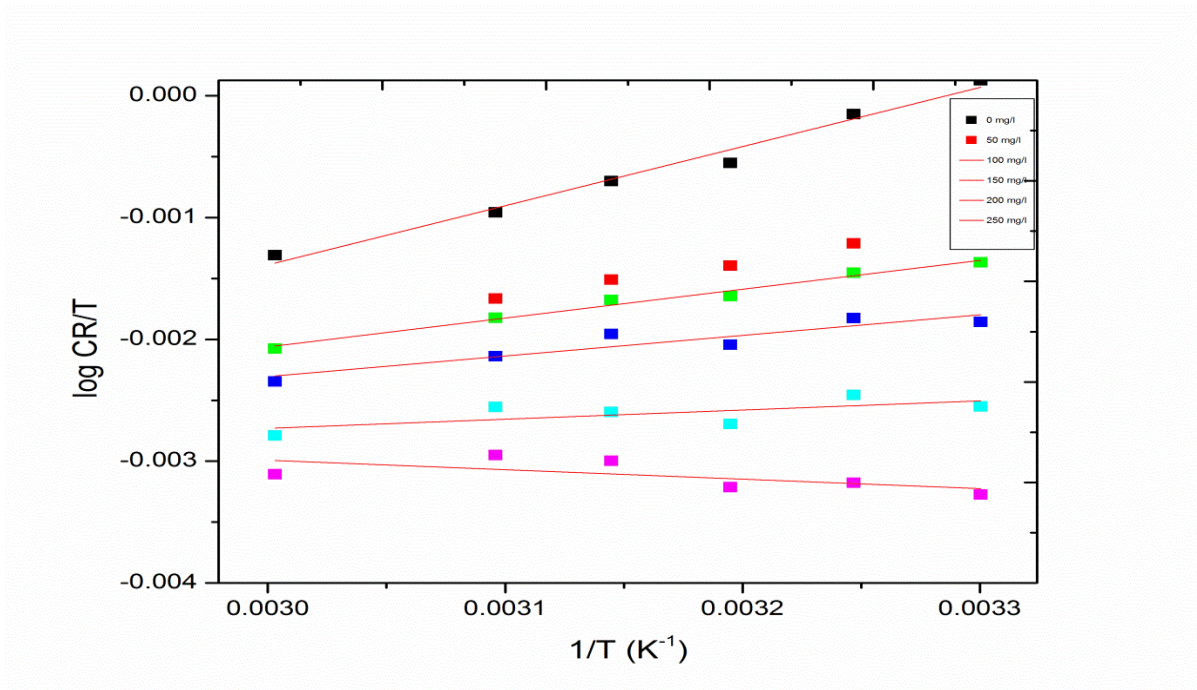
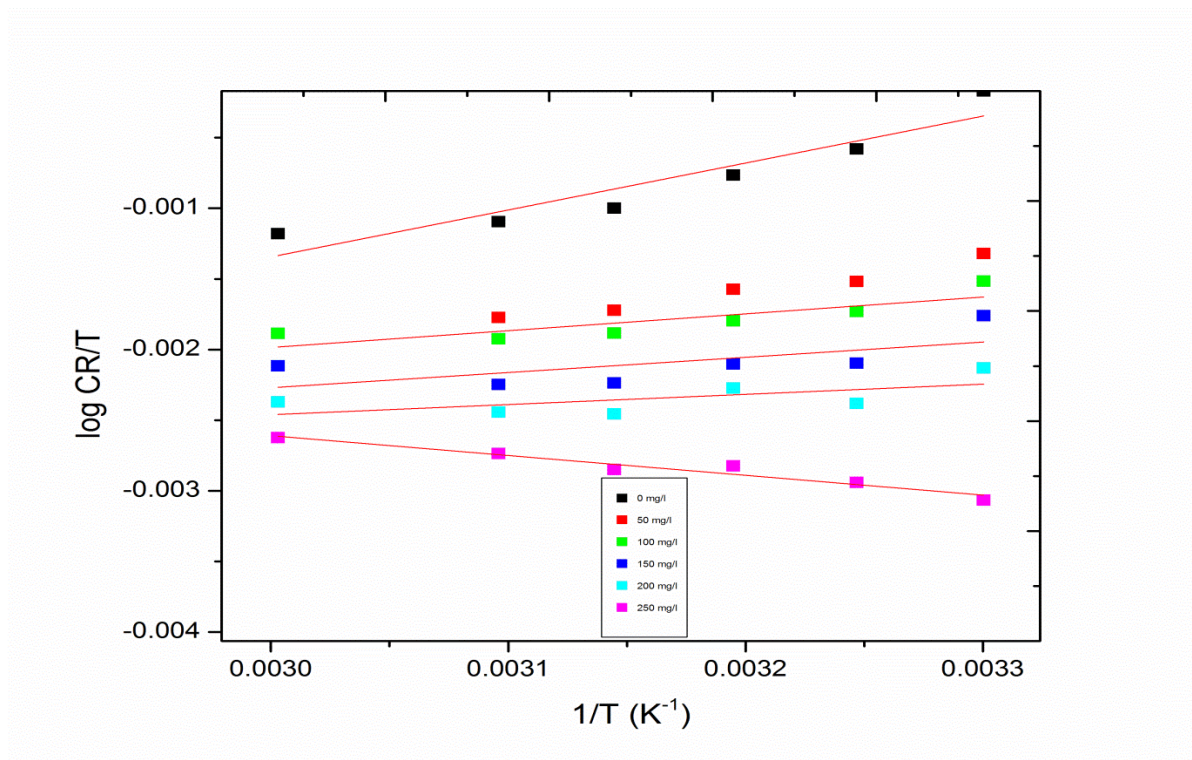


Figure .19. Transition plot for low carbon steel immersed in 1M HCl with and without mixed inhibitor



**Figure .20. Transition plot for low carbon steel immersed in 1M H<sub>2</sub>SO<sub>4</sub> with and without mixed inhibitor**

Where CR is the rate of corrosion, A is the exponential factor, h is the planck's constant, N is the Avagadro's number, E<sub>a</sub> is the activation energy, R is gas constant and T is the absolute temperature.

A plot of logCR vs 1/T gave a straight line with the intercept (logCR) and slope of (-E<sub>a</sub>/2.303R) are shown in the Fig (17)& (18). The values of activation energy in the presence of inhibitor are higher than in its absence and it can be clearly indicates that the presence of mixed inhibitor could be interpreted as physical adsorption [47]. A plot of logCR/T vs 1/T gave a straight line with a slope (-ΔH\*/2.303R) and a intercept (log R/Nh + ΔS\*/2.303R) are shown in fig (6.19) & (6.20). The values of ΔH\* and ΔS\* were calculated and listed in table (7) & (8). The positive sign of ΔH\* in both the 1MHCl and 1MH<sub>2</sub>SO<sub>4</sub> indicates that the endothermic nature of the low carbon steel dissolution process and it can be suggested that the dissolution reaction was slow in the presence of inhibitor [48]. The value ΔS\* in the absence and presence of inhibitor were negative in both 1MHCl and 1MH<sub>2</sub>SO<sub>4</sub>, which can signify that the activated Complex in the rate determining step represent an association rather than dissociation step, meaning that a decrease in disordering takes place on going from reactant to the activated complex [49-51].

## 7. FTIR Studies

The FTIR spectrum of mixed inhibitor (Gutle +TTLE) and the protective film formed on the surface of the metal is shown in Fig .21(a) & 21 (b) respectively. In Fig .21(a),it was found that O-H Stretch at  $3402\text{cm}^{-1}$  was shifted to  $3502\text{cm}^{-1}$  and the aromatic C=C stretch was found at  $1600\text{cm}^{-1}$ .In Fig.21(b) the band at  $2432\text{cm}^{-1}$  was found on S-H stretching vibration. The peak at  $2235\text{cm}^{-1}$  was due to the stretching mode of  $\text{C}\equiv\text{C}$  stretching vibration. The band at approximately  $600\text{-}800\text{cm}^{-1}$  was due to the presence of halogen compounds. The FTIR study leads to the conclusion that adsorption of  $\text{Fe}^{2+}$ (Gutle +TTLE)inhibitor complex formed on the surface of low carbon steel.

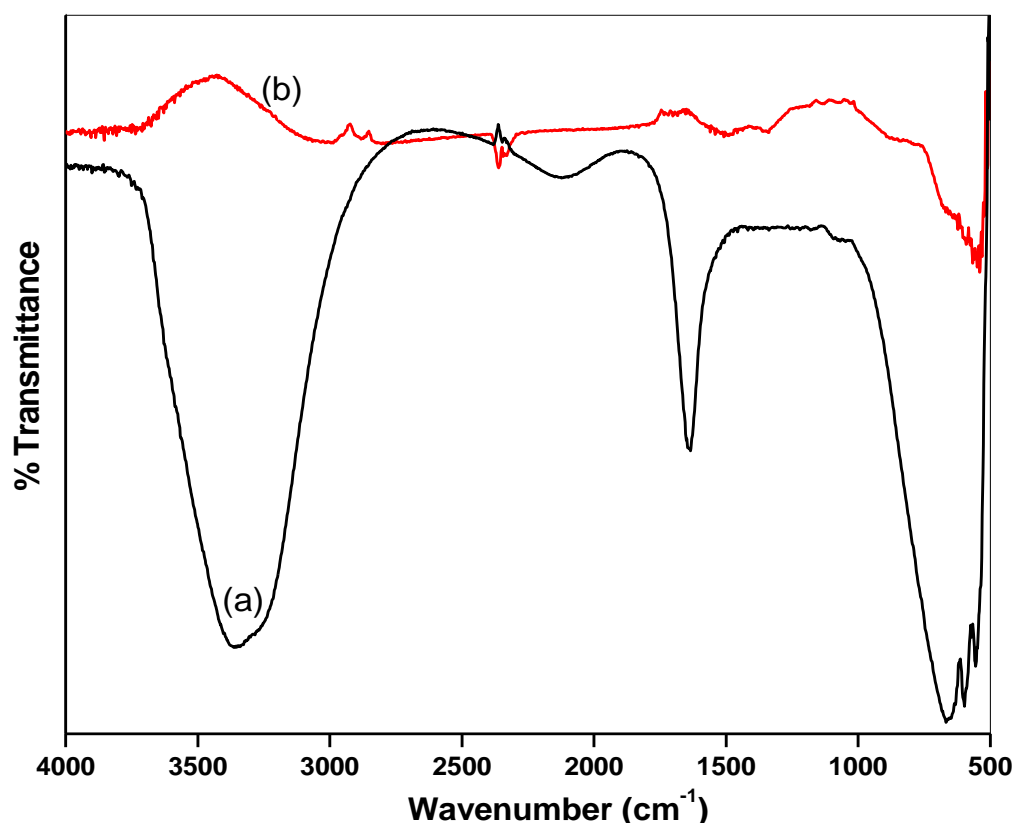


**Figure .21.FTIR Spectra of (a)Corroded sample on low carbon steel (b) Adsorbed layer formed on low carbon steel after immersion in acidic medium containing mixed inhibitor**

## 8. SEM Analysis

Polished low carbon steel specimens were immersed in acidic solutions in the absence and presence of 250mg/l mixed inhibitor for 24hrs are shown in Fig .22a.b.It can be seen from Fig.22a that the surface of the low carbon steel was damaged with cracks and appears deep holes in the absence of inhibitors due to metal dissolution in acid solution.Figure.22b.shows the appearance of spongy,smooth low carbon steel surface after addition of mixed inhibitor to the acidic medium.In figure..22b ,can confirmed that smooth surface on the low carbon steel is due to the formation of protective film, which was responsible for inhibition of corrosion

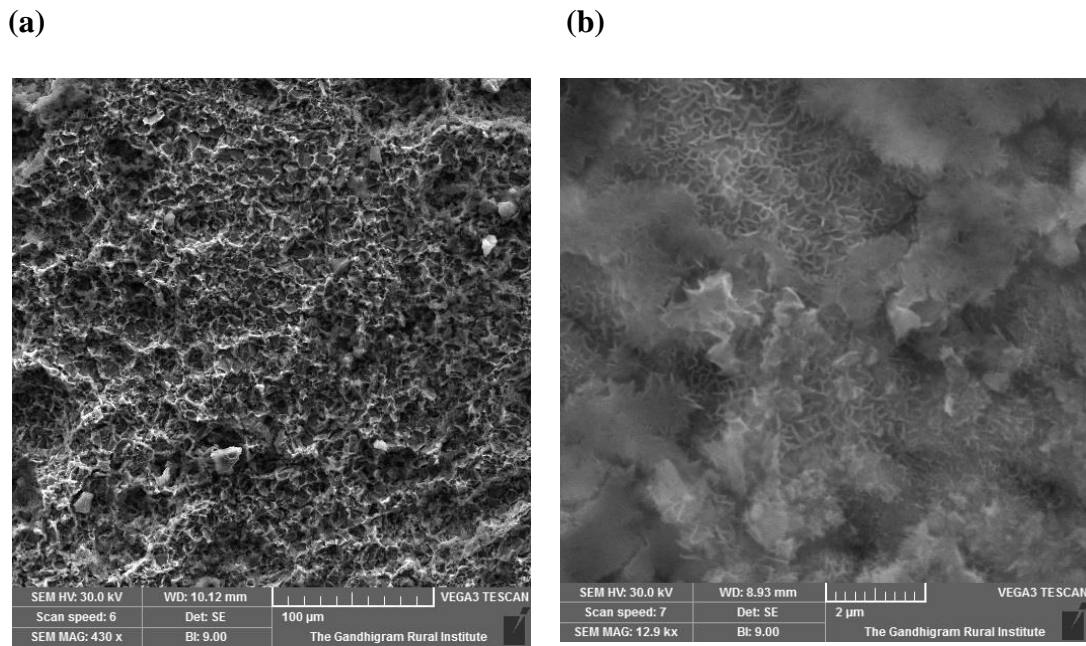


**Figure .22.SEM image of low carbon steel (a) Without inhibitor (b) 250mg/l of Mixed inhibitor**

### 9. EDAX Analysis

The following table -9. shows the EDS spectrum of low carbon steel in acidic solution in the absence and presence of mixed inhibitors. Figure.23.(a) & 23(b) represent EDS spectrum of the corroded sample of the pure low carbon steel and inhibited carbon steel. The spectrum (Fig.23.a.) shows peaks for iron and oxygen suggesting the presence of a iron oxide/hydroxide after corrosion. (Fig.23.b.) shows the peak corresponding to carbon illustrating the presence of inhibitor molecules adsorbed on the metal surface

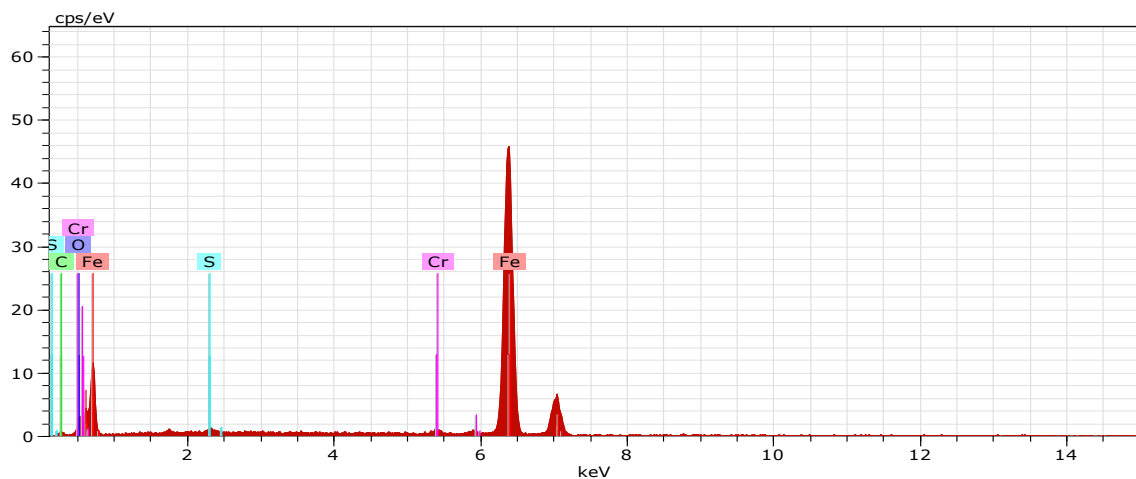


Figure .23.a.EDS Spectrum of corroded sample on low carbon steel

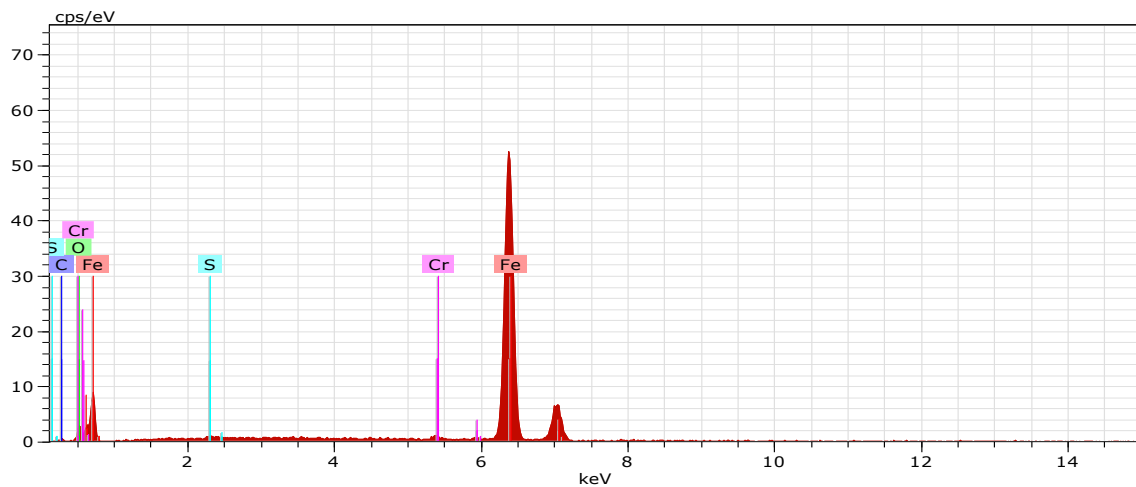


Figure .23.b.EDS spectrum of low carbon steel after treating with mixed inhibitor

Table.9.Surface Composition (weight %) of low carbon steel in absence and presence of mixed inhibitor

Medium	Composition(%)				
	Fe	C	O	S	Cr
Low carbon steel	85.95	5.93	7.04	0.41	0.52
Low carbon steel in mixed inhibitor	80.18	4.33	6.78	0.2	0.51

### 10. UV –Visible spectroscopic Studies

UV-Visible spectroscopy can give the correct evidence on the formation of metal inhibitor complex. The inhibitor contain many components and it is very difficult to separate every compound present in the extract. To confirm the formation of Fe 2+-Mixed inhibitor metal complex,UV-Visible spectra were obtained for pure extract and 1MHCl containing 250mg/l of the extract after 24hrs immersion of Fe2+ at room temperature in Fig.22(a) &.22(b).The electronic absorption spectra of mixed inhibitor showed one sharp band is observed in the UV

region between 300-400nm. The sharp band in the UV region can confirm the presence of various components in the extract. After 24hrs of low carbon steel immersion, there is an high and low level in the absorption band which can confirm that the formation of Fe<sup>2+</sup>-inhibitor complex in the solution.

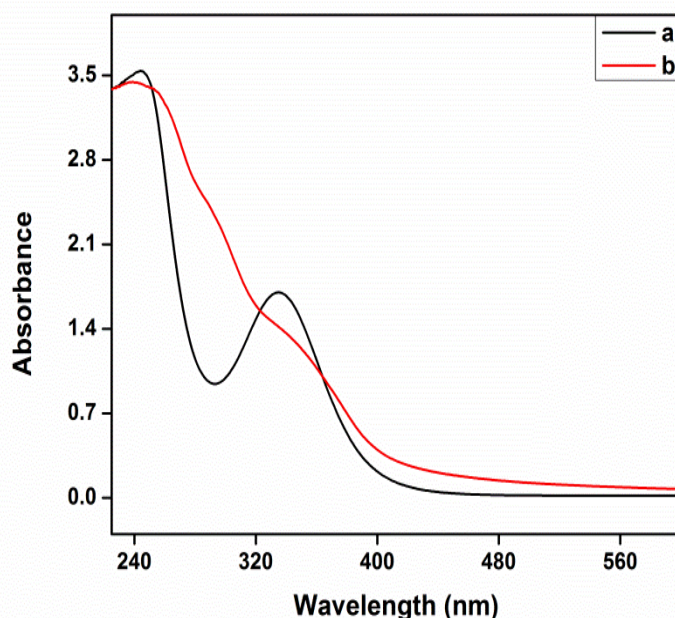


**Figure .22. UV-Visible Spectra of (a) Pure extract (b) Adsorbed layer formed on low carbon steel after immersion in acidic medium containing mixed inhibitor**

## 11. Explanation of inhibition

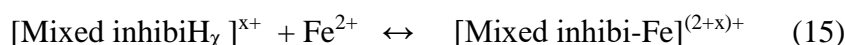
Most of the mixed inhibitors containing natural organic compounds with polar atoms containing N, S, O and P. Low carbon steel is a perfect fit for its Co-ordination affinity to hetero atom bearing ligands [52]. The mixed inhibitor molecules may be adsorbed on the low carbon steel surface can be explained on the basis of the donor-acceptor interaction between  $\pi$ -electron of donor atoms N and aromatic rings of the inhibitors. [53].

From the experimental data, the inhibitive effect of mixed inhibitor (Gutle+ TTLE) in HCl and H<sub>2</sub>SO<sub>4</sub> can be explained as follows.



In acidic solutions, the mixed inhibitor exists either as neutral molecules or in the form of cations. The inhibitor extract may adsorbed on the low carbon steel surface via. The chemical adsorption mechanism, involving the Co-ordinate bonds that can be formed between the empty vacant d-orbitals of Fe atom and the lone electron pairs of the unprotonated N atoms which enhanced the combination between the inhibitor molecules and the electrode surface.

Thus the metal complexes of mixed inhibitor and Fe<sup>2+</sup> or protonated mixed inhibitor might be formed as follows.



Similar type of mechanism was also proved and these complexes might be adsorbed on the low carbon steel surface by Vander waals force to form a protective film to prevent the metal from corrosion.

## 12. Conclusion

Mixed inhibitor extract acts as a very good, environment friendly inhibitor for the corrosion of low carbon steel in 1MHCl and 1MH<sub>2</sub>SO<sub>4</sub>.

Inhibition efficiency increases with increase in inhibitor concentration and shows maximum efficiency in 1MHCl (90%) & 1MH<sub>2</sub>SO<sub>4</sub> (86%) at its optimum concentration (250mg/l).

Inhibition efficiency decreases with the increase in temperature from 303K to 333K.

Polarization studies revealed that E<sub>corr</sub> shifted in the noble directions and the corrosion current decreased with increasing the inhibitor concentration indicated the formation of a protective film by the inhibitors molecule

The adsorption of inhibitor extract on low carbon steel surface follows Langmuir adsorption isotherm.

The inhibitor extract acts as a mixed-type inhibitor in both the acidic medium and the inhibition of the extract on low carbon steel is caused by geometric blocking effect.

UV-Visible and FTIR spectroscopic studies shows that the formation of metal-inhibitor complex which is in good agreement with the anti-corrosive activity of the leaves extract.

SEM reveals the formation of a smooth surface on low carbon steel in the presence of mixed inhibitor extract and it is due to the formation of an adsorptive film of electrostatic character.

## 13. References

Zhang, Q.B., Hua, Y.X.,( 2009). *Electrochem. Acta.* 54, 1881–1887.

Ozkar, D., Kayakırlmaz, K., Bayol, E., Ali Gürten, A. and Kandemirli F. (2012)., *Corros. Sci.* 56: 143–152.

Safak, S., Duran, B., Yurt, A. and Türkoğlu, G. (2012). *Corros. Sci.* 54: 251–259.

Lebrini, M., Robert, F., Lecante, A., Ross, C., (2011). *Corros. Sci.* 53, 687–695

Sorkhabi HA, Asghari E (2008). *Electrochim Acta* 54:162–167.

Oguzie EE (2008) *Mater Chem Phys* 99:441–446.

Okafor PC, Ikpi ME, Uwah IE, Ebenso EE, Ekpe UJ, Umoren SA (2008) .*Corr Sci* 50:2310–2317.

Ismail KM (2007). *Electrochim Acta* 52:7811–7819.

Lebrini M, Robert F, Roos C (2010) .*Int J Electrochem Sci* 5:1698–1712.

Afia L, Salghi R, Bammou L, Bazzi Lh, Hammouti B, Bazzi L (2012) *Acta Metall Sin (Eng Letters)* 25:10–18.

Lahhit N, Bouyanzer A, Desjobert JM, Hammouti B, Salghi R, Costa J, Jama C, Bentiss F, Majidi L (2011) .*Portugaliae Electrochimica Acta* 29:127–138.

Vinodkumar KP, Sangaranarayanapillai M, Rexinthusnavis G (2011) .*J Mater Sci Technol* 27(12):1143–1149.

Goncalves, R.S., Mello, L.D., (2001). *Corros. Sci.* 43, 457–470.

Amin, M.A., El-Sherbini, S.S.A., Bayoumy, R.S., (2007). *Electrochim. Acta* 52, 3588–3600.

Fallavena, T., Antonow, M., Goncalves, R.S., (2006). *Appl. Surf. Sci.* 253, 566–571.

Zhang, D.Q., Cai, Q.R., Gao, L.X., Lee, K.Y., (2008). *Corros. Sci.* 50, 3615–3621.

Bouyanzer, A., Hammouti, B., Majidi, L., (2006). *Mater. Lett.* 60, 2840–2843

De Souza, F.S., Spinelli, A., (2009). *Corros. Sci.* 52, 642–649.

Moretti, G., Guidi, F., Grion, G., (2004). *Corros. Sci.* 46, 387–403.

Muthukrishnan, P. et al., (2013).*Arabian J.of chem.*.1872.

Singh, A.K., Quraishi, M.A., (2010). *Mater. Chem. Phys.* 123, 666–677.

Musa, A.Y., Mohamed, A.B., Takriff, M.S., Jalgham, R.T.T., (2012).

Sharma S, Parihar PS, Nair RN, Verma PS & Sharma A (2012). *Rasayan Journal of Chemistry*, 5(1) 16-22.

Yadav S, Sharma A, Choudhary G & Sharma MA (2014). *International Journal of Advanced Scientific and Technical Research*, 3(9) 16127-16136.

Nair RN, Sharma S, Sharma IK, Verma PS & Sharma A (2010). *Rasayan Journal of Chemistry*, 3(4) 783-790.

Guddi Choudhary, Arpita Sharma, Monika, Rakesh Kumar Banger and \*Alka Sharma(2015) *Ind. J. Sci. Res. and Tech.* 3(6):12-20

Sanja Martinez, Ivica Stern, (2002). *Appl. Surf. Sci.* 199, 83–89.

Ebenso, E.E., Eddy, N.O., Odiongenyi, A.O., (2009). *Electrochim. Acta* 27, 13–22.

Ebenso, E.E., Hailemichael, Umoren, S.A., Obot, I.B., (2008a). *Int. J. Electrochem. Sci.* 3, 1325–1339.

Bentiss, F., Bouanis, M., Mernari, B., Traisnari, M., Vezin, H., Lagrenee, M., (2007). *Appl. Surf. Sci.* 253, 3696–3704.

Oguzie, E.E., Onuoha, G.N., Onuchukwu, A.I., (2005). *Mater. Chem. Phys.* 89, 305–311.

Ita, B.I., Offiong, O.E., (1999). *Mater. Chem. Phys.* 59, 179–184.

Bouklah, M., Benchat, N., Hammouti, B., Aouniti, A., Kertit, S., (2006). *Mater. Lett.* 60, 1901–1905.

S. Leelavathi, R. Rajalakshmi, *J. Mater. Environ. Sci.* 4(5) (2013) 625-638.

- Musa, A.Y., Mohamed, A.B., Takriff, M.S., Jalgham, R.T.T., 2012. *Res. Chem. Intermed.* 38, 453–461.
- Taleb, I., Mehad, H., 2011. *Int. J. Electrochem. Sci.* 6, 5357–5371.
- Vinod kumar, K.P., Narayanan pillai, M.S., Rexin Thusnavis, G., 2010. *P Electrochim. Acta* 28, 373–383.
- Ibrahim, T., Habbab, M., 2011. *Int. J. Electrochem. Sci.* 6, 5357–5371.
- Senthil Kumar, A N., Tharini, K., Sethuraman, M.G., (2009). *Surf. Rev. Lett.* 16, 141–147
- P. Muthukrishnan B. Jeyaprabha, P. Prakash., (2014). *Int J Ind Chem* 5:5
- Behpour, M., Ghoreishi, S.M., Khayatkashani, M., Soltani, N., (2011). *Corros. Sci.* 53, 2489–2501.
- Muthukrishnan, P. et al., (2013). *Arabian J. of chem.* 1872.
- Bouklah, M., Benchat, N., Hammouti, B., Aouniti, A., Kertit, S., (2006). *Mater. Lett.* 60, 1901–1905.
- Behpour, M., Ghoreishi, S.M., Khayatkashani, M., Soltani, N., (2011). *Corros. Sci.* 53, 2489–2501.
- Li, X.H., Deng, S.D., Fu, H., (2010). *Prog. Org. Coat.* 67, 420–426.
- Soltani, N., Behpour, M., Ghoreishi, H., Naeimi, S.M., (2010). *Corros. Sci.* 52, 1351–1361.
- Obot, I.B., Ebenso, E.E., Zuhair, M. Gasem, (2012). *Int. J. Electrochem. Sci.* 7, 1997–2008.
41. Guan NM, Xueming L, Fei L (2004). *Mater Chem Phys* 86:59–68.
- Soltani, N., Behpour, M., Ghoreishi, H., Naeimi, S.M., (2010). *Corros. Sci.* 52, 1351–1361.
- Gomma, M.K., Wahdan, M.H., (1995). *Mater. Chem. Phys.* 39, 209–213.
- Behpour, M., Ghoreishi, S.M., Khayatkashani, M., Soltani, N., (2011). *Corros. Sci.* 53, 2489–2501.
- Shorky, H., Yuasa, M., Sekine, I., Issa, R.M., El-Baradie, H.Y. and Gomma, G.K. (1998). *Corros. Sci.* 40: 2173.
- A. S. Fouda\*, G. Y. Elewady, K. Shalabi and S. Habouba, *International Journal of Advanced Research* (2014), Volume 2, Issue 3, 817-832.